CHAPTER-4

EFFECTS OF HEAT SOURCE AND RADIATION ON AN UNSTEADY MHD FREE CONVECTION FLOW PAST AN INFINITE HEATED VERTICAL PLATE IN A POROUS MEDIUM IN THE PRESENCE OF THERMAL DIFFUSION

4.1 INTRODUCTION

Flow through porous medium past infinite vertical plate is common in nature and has many applications in engineering and science. A number of workers have investigated such flows and excellent literature on the properties and phenomenon may be found in literature [9, 10, 13 – 15]. For example, Soundalgekar [13] investigated the effects of free convection currents on the oscillatory type boundary layer flow past an infinite vertical plate with constant suction where the plate temperature differs from the free steam temperature.

Recently, attention has been on the effects of transversely applied magnetic field and thermal perturbation on the flow of electrically conducting viscous fluids such as plasma. Various properties associated with the interplay of magnetic fields and thermal perturbation in porous medium past vertical plate find useful applications in astrophysics, geophysical fluid dynamics, and engineering. Researchers in these fields have been conducted by many investigators [1, 3, 4, 6, 8, 11, 12 and 16]. For example, Soundalgekar [12] investigated a two dimensional steady free – convection flow of an incompressible, viscous, electrically conducting fluid past an infinite vertical porous plate with constant suction and plate temperature when the difference between the plate temperature and free stream is moderately large to cause free–convection currents. In another study Israel–Cookey and Sigalo [7] investigated the problem of unsteady MHD past a semi–infinite to vertical plate in an optically thin environment with simultaneous effects of radiation, free–convection parameters and time – dependent suction. Chamka [5] investigated the unsteady convective heat and mass transfer past a infinite permeable moving plate with heat absorption where it was found that increase in Solutal Grashoff number enhanced the concentration buoyancy effects leading to an increase in the velocity. Anand Rao and Sivaiah [2] studied the chemical reaction effects on an unsteady MHD free convective flow past an infinite vertical porous plate with constant suction and heat source. S. R. Vempati *et al.* [18] studied the Soret and Dufour effects on unstedy MHD flow past an infinite vertical porous plate with thermal radiation. I. J. Uwanta *et al.* [17] obtained the analytical solution for MHD fluid flow over a vertical plate with Dufour and Soret effects.

The objective of the present chapter is to examine the effects of Heat source and radiation on unsteady MHD free convection flow past an infinite heated vertical plate in a porous medium in the presence of Soret effect. The equations of continuity, linear momentum, energy, diffusion which govern the flow field, are solved by using Galerkin finite element method. Similarity solutions are then obtained numerically for various parameters entering into the problem and discussed them from the physical point of view.

4.2 FORMULATION OF THE PROBLEM

We consider the unsteady flow of an incompressible viscous, radiating hydro magnetic fluid past an infinite porous heated vertical plate with time – dependent suction in an optically thin environment. The physical model and the coordinate system are shown in figure 1. The x' – axis is taken along the vertical infinite porous plate in the upward direction and the y' – axis normal to the plate.

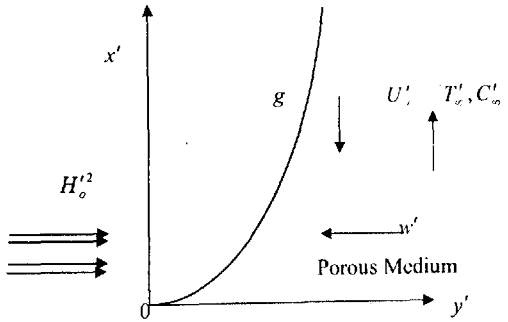

Figure 1. The physical model and coordinate system of the problem

At time $t' = 0$, the plate is maintained at a temperature T_w', which is high enough to initiate radiative heat transfer. A constant magnetic field $H_0'^2$ is maintained in the y' direction and the plate moves uniformly along the positive x' direction with velocity U_0. Under Boussinesq approximation the flow is governed by the following equations:

$$\frac{\partial w'}{\partial y'} = 0 \tag{1}$$

$$\frac{\partial u'}{\partial t'} + w'\frac{\partial u'}{\partial y'} = \upsilon\frac{\partial^2 u'}{\partial y'^2} + \frac{\partial U'}{\partial t'} - \left(\frac{\mu^2\sigma_C H_0'^2}{\rho} + \frac{\upsilon}{K}\right)(u' - U') + g\beta(T' - T'_\infty) + g\beta^*(C' - C'_\infty) \tag{2}$$

$$\frac{\partial T'}{\partial t'} + w'\frac{\partial T'}{\partial y'} = \frac{k}{\rho C_p}\left(\frac{\partial^2 T'}{\partial y'^2} - \nabla q'_{z'}\right) + \frac{\mu}{\rho C_p}\left(\frac{\partial u'}{\partial y'}\right)^2 - \frac{Q_o}{\rho C_p}(T' - T'_\infty) \tag{3}$$

$$\frac{\partial^2 q_{z'}}{\partial y'^2} - 3\alpha^2 q'_{z'} - 16\alpha\,\sigma\,T_\infty^3\frac{\partial T'}{\partial y'} = 0 \tag{4}$$

$$\frac{\partial C'}{\partial t'} + w'\frac{\partial C'}{\partial y'} = D\frac{\partial^2 C'}{\partial y'^2} + \frac{D_m k_T}{T_m}\frac{\partial^2 T'}{\partial y'^2} \tag{5}$$

The boundary conditions are

$$\begin{aligned} &u' = 0,\ T' = T'_w,\ C' = C'_w \ \ on \ \ y' = 0 \\ &u' \to 0,\ T' \to T'_\infty,\ C' \to C'_\infty \ \ as \ \ y' \to \infty \end{aligned} \tag{6}$$

Where (u', v', w'), Dimensional velocity components; (x', y'), Dimensional Cartesian coordinates; $H_0'^2$, Constant transverse magnetic field; w'_0, Dimensional suction velocity; T'_w, Wall temperature; T'_∞, Reference temperature ; U', Dimensional free stream velocity; t', Dimensional time; C'_w, Concentration near the plate; C'_∞, Concentration in the fluid for away from the plate the plate; ρ, Density; g, Acceleration due to gravity; K, Dimensional porosity parameter; C_p, Specific heat capacity; k, Thermal conductivity; q'_z, Radiative heat flux; U_0, Mean velocity of $U'(t')$; σ_c, Electrical conductivity; Q_0, Dimensional heat absorption coefficient; υ, Kinematic coefficient; μ, Permeability; ε, Time corrective parameter; β, Coefficients of volume expansion due to temperature; β^*, Coefficient of volume expansion due to concentration; D, Chemical diffusivity; D_m, Molecular diffusivity;

k_T, Mean absorption coefficient; T_m, Mean fluid temperature; α^2, Absorption coefficient; ω', Dimensional free stream frequency of oscillation

Since the medium is optically thin with relatively low density and $\alpha << 1$ the radiative heat flux given by equation (4) in the spirit of Cogley *et al.* [6] becomes

$$\frac{\partial q'_r}{\partial y'} = 4\alpha^2 (T' - T'_\infty) \tag{7}$$

$$\text{Where } \alpha^2 = \int_0^\infty \delta\lambda \frac{\partial B}{\partial T'} \tag{8}$$

Here B is the Planks constant, δ is the radiation absorption and λ is the frequency.

Further, from equation (1) it is clear that the suction velocity w' at the plate is either a constant or a function of time only. So we assume it in the form

$$w' = -w'_0 \left(1 + \varepsilon A e^{i\omega' t'}\right) \tag{9}$$

Where A Small positive parameter, and ε is small such that $\varepsilon A << 1$, and the negative sign indicates that the suction velocity is towards the plate.

In view of equations (4), (8) and (9), equations (2), (3) and (5) become

$$\frac{1}{4}\frac{\partial u}{\partial t} - \left(1 + \varepsilon A\, e^{i\omega t}\right)\frac{\partial u}{\partial y} = \frac{1}{4}\frac{\partial U}{\partial t} + \frac{\partial^2 u}{\partial y^2} - (M^2 + \chi^2)(u - U) + Gr\theta + GcC \tag{10}$$

$$\frac{1}{4}\Pr\frac{\partial \theta}{\partial t} - \Pr\left(1 + \varepsilon A\, e^{i\omega t}\right)\frac{\partial \theta}{\partial y} = \left(\frac{\partial^2}{\partial y^2} - R^2\right)\theta + \Pr Ec\left(\frac{\partial u}{\partial y}\right)^2 - \Pr S\theta \tag{11}$$

$$\frac{1}{4}Sc\frac{\partial C}{\partial t} - Sc\left(1 + \varepsilon A\, e^{i\omega t}\right)\frac{\partial C}{\partial y} = \frac{\partial^2 C}{\partial y^2} + (Sr)(Sc)\left(\frac{\partial^2 \theta}{\partial y^2}\right) \tag{12}$$

Where we used the following non-dimensional variables and parameters.

$$\left.\begin{array}{l} t=\dfrac{w_0'^2 t'}{4\upsilon},\quad y=\dfrac{w_0' y'}{\upsilon},\quad u=\dfrac{u'}{U_0},\quad \omega=\dfrac{4\upsilon\omega'}{w_0'^2},\quad U=\dfrac{U'}{U_0},\quad \theta=\dfrac{T'-T'_\infty}{T'_w-T'_\infty}, \\ \Pr=\dfrac{\mu c_p}{k},\quad Gr=\dfrac{g\beta\upsilon(T'_w-T'_\infty)}{U_0 w_0'^2},\quad Gc=\dfrac{g\beta^*\upsilon(C'_w-C'_\infty)}{U_0 w_0'^2},\quad Ec=\dfrac{U_0^2}{C_p(T'_w-T'_\infty)}, \\ R^2=\dfrac{4\alpha^2}{\rho C_p k w_0'^2}(T'_w-T'_\infty),\ S=\dfrac{\upsilon Q_0}{\rho c_p w_0'^2},\quad M^2=\dfrac{\mu^2\sigma_C H_0'^2}{\upsilon\rho w_0'^2}, \\ Sr=\dfrac{D_m k_T(T'_w-T'_\infty)}{\upsilon T_m(C'_w-C'_\infty)},\ Sc=\dfrac{\upsilon}{D},\ C=\dfrac{(C'-C'_\infty)}{(C'_w-C'_\infty)},\ \chi^2=\dfrac{\upsilon^2}{K w_0'^2}. \end{array}\right\} \quad (13)$$

Where M^2, Hartmann number; Pr, Prandtl number; Sc, Schmidt number; Ec, Eckert number; θ, Non–dimensional temperature; C, Non – dimensional species concentration; Gr, Grashof number; Gc, Modified Grashof number; χ^2, Darcy number (Non dimensional permeability parameter); S_r, Soret number; R^2, Radiation parameter; S, Heat source.

Equations (10), (11) and (12) are now subject to the boundary conditions

$$\left.\begin{array}{l} u=0,\quad \theta=1, C=1 \ on \ y=0 \\ u\to 0,\ \theta\to 0, C\to 0 \ as \ y\to\infty \end{array}\right\} \quad (14)$$

The mathematical statement of the problem is now complete and embodies the solution of equations (10), (11) and (12) subject to boundary conditions (14).

4.3 METHOD OF SOLUTION

By applying Galerkin finite element method for equation (10) over the element (e), $(y_j \le y \le y_k)$ is:

$$\int_{y_j}^{y_k}\left\{N^{(e)T}\left[4\frac{\partial^2 u^{(e)}}{\partial y^2}-\frac{\partial u^{(e)}}{\partial t}+4B\frac{\partial u^{(e)}}{\partial y}-Du^{(e)}+P\right]\right\}dy=0 \quad (15)$$

Where $P=\dfrac{\partial U}{\partial t}+4(Gr)\theta+4(Gc)C+DU$, $B=1+\varepsilon A e^{i\omega t}$, $D=4(M^2+\chi^2)$;

Integrating the first term in equation (15) by parts one obtains

$$4N^{(e)T}\left\{\frac{\partial u^{(e)}}{\partial y}\right\}_{y_j}^{y_k} - \int_{y_j}^{y_k}\left\{4\frac{\partial N^{(e)T}}{\partial y}\frac{\partial u^{(e)}}{\partial y} + N^{(e)T}\left(\frac{\partial u^{(e)}}{\partial t} - 4B\frac{\partial u^{(e)}}{\partial y} + Du^{(e)} - P\right)\right\}dy = 0 \qquad (16)$$

Neglecting the first term in equation (16), one gets:

$$\int_{y_j}^{y_k}\left\{4\frac{\partial N^{(e)T}}{\partial y}\frac{\partial u^{(e)}}{\partial y} + N^{(e)T}\left(\frac{\partial u^{(e)}}{\partial t} - 4B\frac{\partial u^{(e)}}{\partial y} + Du^{(e)} - P\right)\right\}dy = 0$$

Let $u^{(e)} = N^{(e)}\phi^{(e)}$ be the linear piecewise approximation solution over the element (e) $(y_j \le y \le y_k)$ where $N^{(e)} = [N_j \quad N_k]$, $\phi^{(e)} = [u_j \quad u_k]^T$ and $N_j = \frac{y_k - y}{y_k - y_j}, N_k = \frac{y - y_j}{y_k - y_j}$ are the basis functions. One obtains:

$$4\int_{y_j}^{y_k}\left\{\begin{bmatrix} N_j' N_j' & N_j' N_k' \\ N_j' N_k' & N_k' N_k' \end{bmatrix}\begin{bmatrix} u_j \\ u_k \end{bmatrix}\right\}dy + \int_{y_j}^{y_k}\left\{\begin{bmatrix} N_j N_j & N_j N_k \\ N_j N_k & N_k N_k \end{bmatrix}\begin{bmatrix} \dot{u}_j \\ \dot{u}_k \end{bmatrix}\right\}dy - 4B\int_{y_j}^{y_k}\left\{\begin{bmatrix} N_j N_j' & N_j N_k' \\ N_j' N_k & N_k' N_k \end{bmatrix}\begin{bmatrix} u_j \\ u_k \end{bmatrix}\right\}dy$$

$$+ D\int_{y_j}^{y_k}\left\{\begin{bmatrix} N_j N_j & N_j N_k \\ N_j N_k & N_k N_k \end{bmatrix}\begin{bmatrix} u_j \\ u_k \end{bmatrix}\right\}dy = P\int_{y_j}^{y_k}\begin{bmatrix} N_j \\ N_k \end{bmatrix}dy$$

Simplifying we get

$$\frac{4}{l^{(e)^2}}\begin{bmatrix} 1 & -1 \\ -1 & 1 \end{bmatrix}\begin{bmatrix} u_j \\ u_k \end{bmatrix} + \frac{1}{6}\begin{bmatrix} 2 & 1 \\ 1 & 2 \end{bmatrix}\begin{bmatrix} \dot{u}_j \\ \dot{u}_k \end{bmatrix} - \frac{4B}{2l^{(e)}}\begin{bmatrix} -1 & 1 \\ -1 & 1 \end{bmatrix}\begin{bmatrix} u_j \\ u_k \end{bmatrix} + \frac{D}{6}\begin{bmatrix} 2 & 1 \\ 1 & 2 \end{bmatrix}\begin{bmatrix} u_j \\ u_k \end{bmatrix} = \frac{P}{2}\begin{bmatrix} 1 \\ 1 \end{bmatrix}$$

Where prime and dot denotes differentiation w.r.t y and time t respectively. Assembling the element equations for two consecutive elements $(y_{i-1} \le y \le y_i)$ and $(y_i \le y \le y_{i+1})$, one obtains

$$\frac{4}{l^{(e)^2}}\begin{bmatrix} 1 & -1 & 0 \\ -1 & 2 & -1 \\ 0 & -1 & 1 \end{bmatrix}\begin{bmatrix} u_{i-1} \\ u_i \\ u_{i+1} \end{bmatrix} + \frac{1}{6}\begin{bmatrix} 2 & 1 & 0 \\ 1 & 4 & 1 \\ 0 & 1 & 2 \end{bmatrix}\begin{bmatrix} \dot{u}_{i-1} \\ \dot{u}_i \\ \dot{u}_{i+1} \end{bmatrix} - \frac{4B}{2l^{(e)}}\begin{bmatrix} -1 & 1 & 0 \\ -1 & 0 & 1 \\ 0 & -1 & 1 \end{bmatrix}\begin{bmatrix} u_{i-1} \\ u_i \\ u_{i+1} \end{bmatrix} + \tag{17}$$

$$\frac{D}{6}\begin{bmatrix} 2 & 1 & 0 \\ 1 & 4 & 1 \\ 0 & 1 & 2 \end{bmatrix}\begin{bmatrix} u_{i-1} \\ u_i \\ u_{i+1} \end{bmatrix} = \frac{\dot{P}}{2}\begin{bmatrix} 1 \\ 2 \\ 1 \end{bmatrix}$$

Now put row corresponding to the node i to zero, from equation (17) the difference schemes with $l^{(e)} = h$ is:

$$\frac{4}{h^2}\left[-u_{i-1} + 2u_i - u_{i+1}\right] + \frac{1}{6}\left[\dot{u}_{i-1} + 4\dot{u}_i + \dot{u}_{i+1}\right] - \frac{4B}{2h}\left[-u_{i-1} + u_{i+1}\right] + \frac{D}{6}\left[u_{i-1} + 4u_i + u_{i+1}\right] = P \tag{18}$$

Applying the trapezoidal rule, following system of equations in Crank – Nicholson method are obtained:

$$A_1 u_{i-1}^{n+1} + A_2 u_i^{n+1} + A_3 u_{i+1}^{n+1} = A_4 u_{i-1}^{n} + A_5 u_i^{n} + A_6 u_{i+1}^{n} + P^* \tag{19}$$

Now from equations (11) and (12) following equations are obtained:

$$B_1\theta_{i-1}^{n+1} + B_2\theta_i^{n+1} + B_3\theta_{i+1}^{n+1} = B_4\theta_{i-1}^{n} + B_5\theta_i^{n} + B_6\theta_{i+1}^{n} + Q^* \tag{20}$$

$$C_1 C_{i-1}^{n+1} + C_2 C_i^{n+1} + C_3 C_{i+1}^{n+1} = C_4 C_{i-1}^{n} + C_5 C_i^{n} + C_6 C_{i+1}^{n} + R^{**} \tag{21}$$

Where

$A_1 = 2 + 12Brh + Dk - 24r,\ A_2 = 8 + 4Dk + 48r,\ A_3 = 2 - 12Brh + Dk - 24r,$

$A_4 = 2 - 12Brh - Dk + 24r,\ A_5 = 8 - 4Dk - 48r,\ A_6 = 2 + 12Brh + Dk + 24r,$

$B_1 = 2(\Pr) + 12(\Pr)Brh + 4R^2k - 24r + 4S(\Pr)k,\ B_2 = 8(\Pr) + 48r + 16R^2k + 16S(\Pr)k,$

$B_3 = 2(\Pr) - 12(\Pr)Brh + 4R^2k - 24r + 4S(\Pr)k,\ B_4 = 2(\Pr) - 12(\Pr)Brh - 4R^2k + 24r - 4S(\Pr)k,$

$B_5 = 8(\Pr) - 48r - 16R^2k - 16S(\Pr)k,\ B_6 = 2(\Pr) + 12(\Pr)Brh - 4R^2k + 24r - 4S(\Pr)k,$

$C_1 = 2(Sc) + 12(\Pr)Brh - 24r,\ C_2 = 8(Sc) + 48r,\ C_3 = 2(Sc) - 12(Sc)Brh - 24r,$

$C_4 = 2(Sc) - 12(Sc)Brh + 24r,\ C_5 = 8(Sc) - 48r,\ C_6 = 2(Sc) + 12(Sc)Brh + 24r,$

$$P^{*} = 12Pk = 12k\left(\frac{\partial U}{\partial t} + 4(Gr)\theta + 4(Gc)C + DU\right),\ Q^{*} = 12Qk = 48(\Pr)k(Ec)\left(\frac{\partial u}{\partial y}\right)^{2},$$

$$R^{**} = 12R^{*}k = 48(Sc)(Sr)k\left(\frac{\partial^{2}\theta}{\partial y^{2}}\right);$$

Here r = $\frac{k}{h^2}$ and h, k are mesh sizes along y–direction and time–direction respectively. Index i refers to space and j refers to the time. In the equations (19), (20) and (21), taking $i = 1(1)n$ and using boundary conditions (14), then the following system of equations are obtained:

$$A_i X_i = B_i \quad i = 1(1)3 \tag{22}$$

where $A_i^{'}$s are matrices of order n and $X_i, B_i^{'}$s are column matrices having n – components. The solutions of above system of equations are obtained by using Thomas algorithm for velocity, temperature and concentration. Also, numerical solutions for these equations are obtained by C – programme. In order to prove the convergence and stability of Galerkin finite element method, the same C – programme was run with smaller values of h and k no significant change was observed in the values of u, θ and C. Hence the Galerkin finite element method is stable and convergent.

4.4 DISCUSSION OF THE RESULTS

In the previous sections, we have formulated and solved the problem of an unsteady MHD free convection flow past an infinite heated vertical plate in a porous medium with radiation. By invoking, the optically thin differential approximation for the radiative heat flux in the energy equation. In the numerical computation, the Prandtl number ($\Pr = 0.71$) which corresponds to air and various values of the material parameters are used. In addition, the boundary condition $y \to \infty$ is approximated by $y_{max} = 2$, which is sufficiently large for the velocity to approach the relevant stream velocity. The temperature and the species concentration are coupled to the velocity via Grashof number (Gr) and Modified Grashof number (Gc) as seen in equation (9). For various values of Grashof number and Modified

Grashof number, the velocity profiles u are plotted in figures (2) and (3). The Grashof number (Gr) signifies the relative effect of the thermal buoyancy force to the viscous hydrodynamic force in the boundary layer. As expected, it is observed that there is a rise in the velocity due to the enhancement of thermal buoyancy force. Also, as (Gr) increases, the peak values of the velocity increases rapidly near the porous plate and then decays smoothly to the free stream velocity. The Modified Grashof number (Gc) defines the ratio of the species buoyancy force to the viscous hydrodynamic force. As expected, the fluid velocity increases and the peak value is more distinctive due to increase in the species buoyancy force. The velocity distribution attains a distinctive maximum value in the vicinity of the plate and then decreases properly to approach the free stream value. It is noticed that the velocity increases with increasing values of Modified Grashof number(Gc). Figure (4) illustrate the velocity profiles for different values of Prandtl number Pr. The numerical results show that the effect of increasing values of Prandtl number result in decreasing velocity. The nature of velocity profiles in presence of foreign species such as Hydrogen (Sc = 0.22), Helium (Sc = 0.22), Water vapour (Sc = 0.60) and Oxygen (Sc = 0.66) are shown in figure (5). The flow field suffers a decrease in primary velocity at all points in presence of heavier diffusing species. The effect of the magnetic field parameter M is shown in figure (6) in case of cooling of the plate. It is observed that the velocity of the fluid decreases with the increase of the magnetic field parameter values. The decrease in the velocity as the Hartmann number M increases is because the presence of a magnetic field in an electrically conducting fluid introduces a force called the Lorentz force, which acts against the flow if the magnetic field is applied in the normal direction, as in the present study. This resistive force slows down the fluid velocity component as shown in figure (6). The influence of the viscous dissipation parameter i.e., the Eckert number Ec on the velocity and temperature are shown in figures (7) and (13) respectively. The Eckert number Ec expresses the relationship between the kinetic energy in the flow and the enthalpy. It embodies the conversion of kinetic energy into internal energy by work done against the viscous fluid stresses. Greater viscous dissipative heat causes a rise in the temperature as well as the velocity.

The effect of the thermal radiation parameter R on the primary velocity and temperature profiles in the boundary layer are illustrated in figures (8) and (15) respectively. Increasing the thermal radiation parameter R produces significant increase in the thermal condition of the fluid and its thermal boundary layer. This increase in the fluid temperature induces more flow in the boundary layer causing the velocity of the fluid there to increase. Figure (9) and (14) has been plotted to depict the variation of velocity and temperature profiles against y for different values of heat source parameter S by fixing other physical parameters. From this Graph we observe that velocity and temperature decrease with increase in the heat source parameter S because when heat is absorbed, the buoyancy force decreases the temperature profiles. Figure (10) shows the effects of Darcy number χ on the velocity profiles for cooling as well as heating of the plate. For a cooling plate fluid velocity increases, whereas for a heating plate it decreases with increase of χ. Darcy number is the measurement of the porosity of the medium. As the porosity of the medium increases, the value of χ increases. For large porosity of the medium fluid gets more space to flow as a consequence its velocity increases. The variations of tangential velocity distribution with y for different values of the Soret number (Sr) are shown in figure (11). It can be clearly seen that the velocity distribution in the boundary layer increases with the Soret number. Figure (12) illustrate the temperature profiles for different values of Prandtl number $\Pr$. It is observed that the temperature decrease as an increasing the Prandtl number. The reason is that smaller values of Pr are equivalent to increase in the thermal conductivity of the fluid and therefore heat is able to diffuse away from the heated surface more rapidly for higher values of Pr. Hence in the case of smaller Prandtl number the thermal boundary layer is thicker and the rate of heat transfer is reduced. The effects of Schmidt number (Sc) and Soret number (Sr) on the concentration field are presented in figures (16) and (17). Figure (16) shows the concentration field due to variation in Schmidt number (Sc) for the gasses Hydrogen, Helium, Water – vapour, Oxygen and Ammonia. It is observed that concentration field is steadily for Hydrogen and falls rapidly for Oxygen and Ammonia in comparison to Water – vapour. Thus Hydrogen can be used for maintaining effective concentration field and Water – vapour can be used for maintaining normal concentration field. In figure (17), it is observed that an increase in the Soret number (Sr) leads to increase in the concentration field.

OBSERVATIONS:

In conclusion therefore, the flow of an unsteady MHD free convection past an infinite heated vertical plate in a porous medium under the simultaneous effects of viscous dissipation, radiation and heat source is affected by the material parameters. The governing equations are approximated to a system of linear partial differential equations by using Galerkin finite element method. The results are presented graphically and we can conclude that the flow field and the quantities of physical interest are significantly influenced by these parameters.

1. The velocity increases as Grashof number Gr, Modified Grashof number Gc, Eckert number, Thermal radiation parameter R, Darcy parameter χ , Ec and Soret number Sr increases. However, the velocity was found to decreases as the Hartmann number M, Prandtl number Pr, Schmidt number Sc, and Heat source parameter S are increases.
2. The fluid temperature was found to decreases as the Heat source parameter S and Prandtl number Pr are increases and found to increase as Eckert number Ec, and thermal radiation parameter R are increases.
3. The fluid concentration was found to decreases as the Schmidt number Sc and increases as the Soret number Sr increases.

4.5 REFERENCES

[1] Alagoa, K. D., G. Tay, T. M. Abbey, Radiative and free – convection effects of MHD through porous medium between infinite parallel plates with time – dependent suction, *Astrophys. Space Sci.*, 260, 455 – 468 (1999).

[2] Anand Rao .J and Shivaiah. S, Chemical reaction effects on an unsteady MHD free convective flow past an infinite vertical porous plate with constant suction and heat source, *International Journal of Applied Mathematics and Mechanics*, 7(8), 98 – 118 (2011).

[3] Bestman, A. R., S. K. Adjepong, Unsteady hydromagnetic free – convection flow with radiative heat transfer in a rotating fluid, *Astrophys. Space Sci.*, 143, 73 – 80 (1998).

[4] Bestman, A. R., Transient effect on laminar convection to a radiating gas past a vertical flat plate, *AMSE Modell. Simul. Control B*, 3(2), 1 – 10 (1985).

[5] Chamkha A.J., Unsteady MHD Convective Heat and Mass Transfer Past a Semi-infinite Vertical Permeable Moving Plate with Heat Absorption, *Int. J. Eng. Sci.*, 42, 217 – 230 (2004).

[6] Cogley, A. C. L., W. G. Vincenti, E. S. Gillies, Differential approximation for radiative heat transfer in a non – linear equations – grey gas near equilibrium, *Am. Inst. Aeronuat. Astronaut. J.*, 6, 551 – 553 (1968).

[7] Israel – Cookey, C., F. B. Sigalo, On the unsteady MHD free convection flow past infinite heated porous vertical plate with time dependent suction and radiative heat transfer, *Amse. Modell. Meas. Control in press.*

[8] Kim, Y. J., Unsteady MHD convective heat transfer past a semi-infinite vertical porous moving plate with variable suction, *Int. J. Engng. Sci.*, 38, 833 – 845 (2000).

[9] Lightill, M. J., The response of laminar skin – friction and heat transfer fluctuations in the stream velocity, *Proc. Royal Soc. London A*, 224, 1 – 23 (1954).

[10] Pop, I., V. M. Soundalgekar, On the unsteady boundary layers in a rotating flow, *J. Inst. Maths Applica.*, 15, 343 – 349 (1975).

[11] Singh, A. K., C. K. Dikshif, Hydromagnetic flow past a continuously moving semi–infinite plate at large suction, *Astrophys. Space Sci.*, 248, 249–256 (1988).

[12] Soundalgekar, V. M., Free – convection effects on steady MHD flow past a vertical porous plate, *J. Fluid Mech.*, 66, 41 – 55 (1974).

[13] Soundalgekar, V. M., Free – convection effects on the oscillatory flow past an infinite vertical porous plate with constant suction I, *Proc. Royal Soc. London A*, 333, 25 – 36 (1973).

[14] Soundalgekar, V. M., Free – convection effects on the oscillatory flow past an infinite vertical porous plate with constant suction II, *Proc. Royal Soc. London A*, 333, 37 – 50 (1973).

[15] Stuart, T. J., A solution of the Navier – Stokes and energy illustrating the response of skin – friction and temperature of an infinite plate thermometer to fluctuations in the stream velocity, *Proc. Royal Soc. London A*, 231, 116 – 130 (1955).

[16] Takhar, H. S., R. S. R. Gorla, V. M. Soundalgekar, Radiative effects on MHD free – convection flow past a semi – infinite vertical plate, *Int. J. Number. Heat Fluid Flow*, 6(2), 77 – 83 (1996).

[17] I. J. Uwanta, K. K. Asogwa, U. A. Ali, The analytical solution for MHD fluid flow over a vertical plate with Dufour and Soret effects *Int.J.Comp.Appl.* 45(2), 8-16 (2012).

[18] S. R. Vempati , A. B. Lakshminarayana-Gari, The Soret and Dufour effects on unstedy MHD flow past an infinite vertical porous plate with thermal radiation. *Appl. Math. Mech. Engl. Ed.*, 31(12), 1481-1496 (2010).

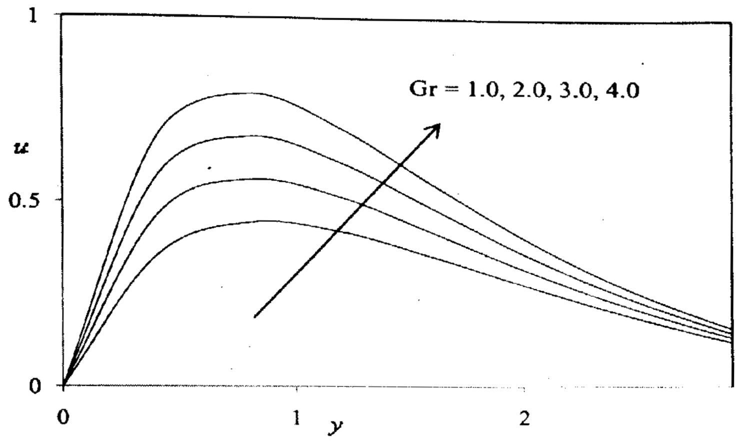

Figure 2. Velocity profiles for different values of Gr

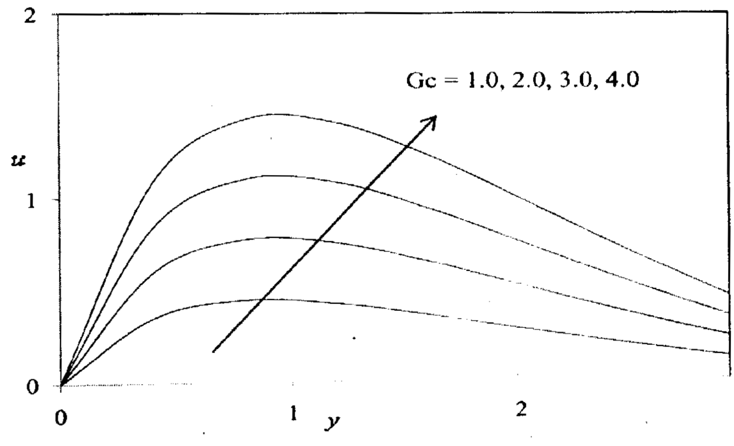

Figure 3. Velocity profiles for different values of Gc

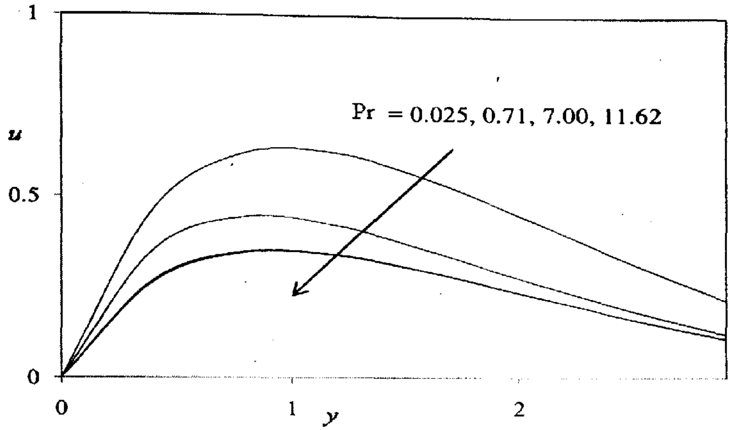

Figure 4. Velocity profiles for different values of Pr

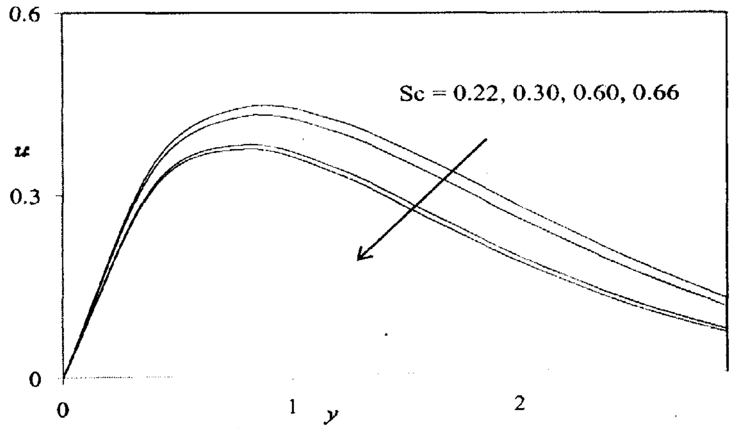

Figure 5. Velocity profiles for different values of Sc

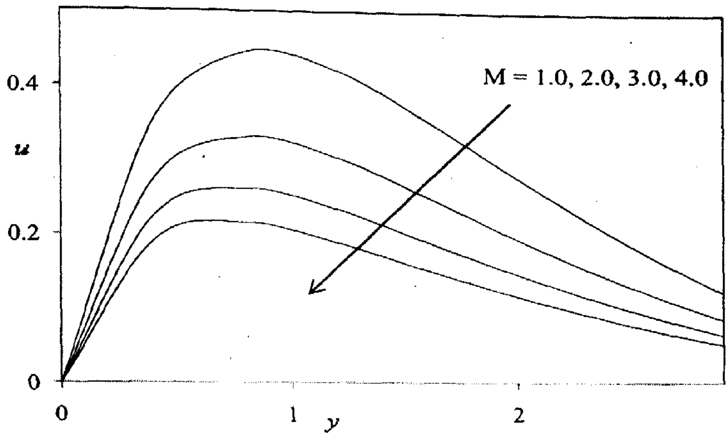

Figure 6. Velocity profiles for different values of M

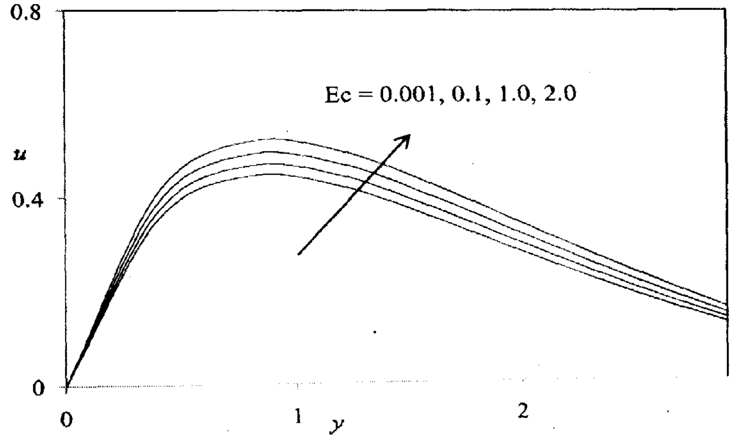

Figure 7. Velocity profiles for different values of Ec

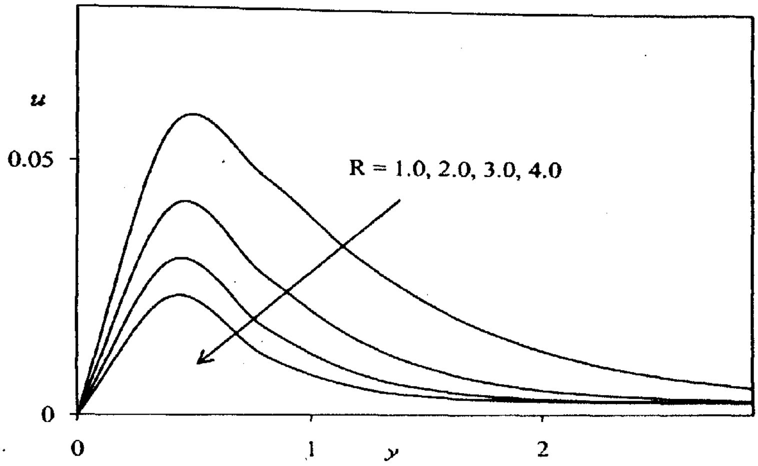

Figure 8. Velocity profiles for different values of R

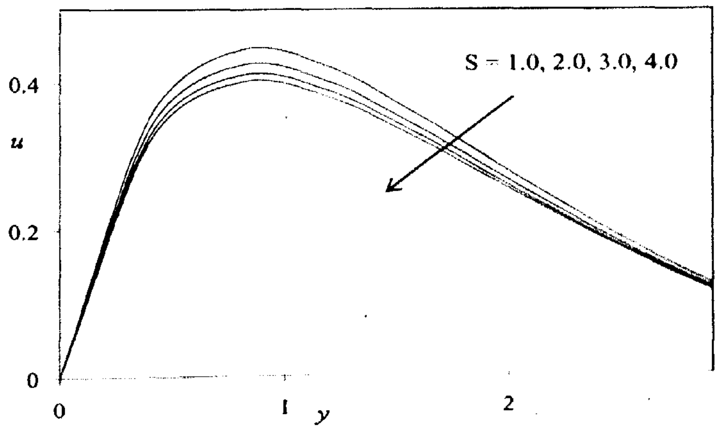

Figure 9. Velocity profiles for different values of S

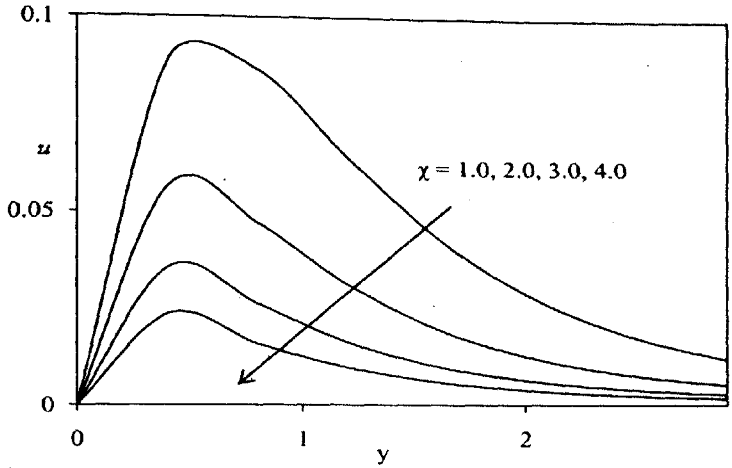

Figure 10. Velocity profiles for different values of χ

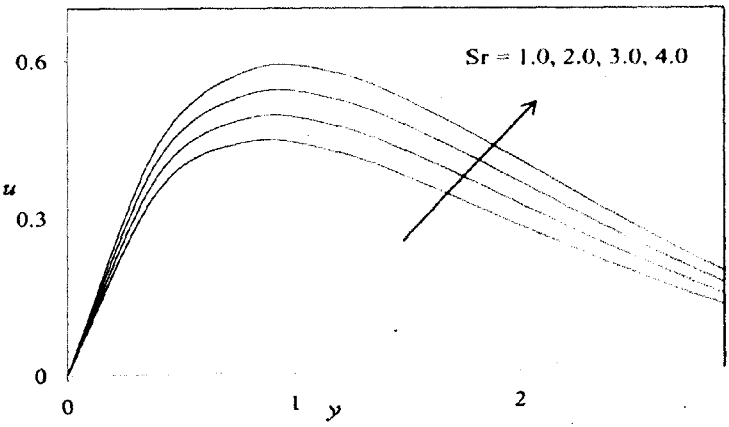

Figure 11. Velocity profiles for different values of Sr

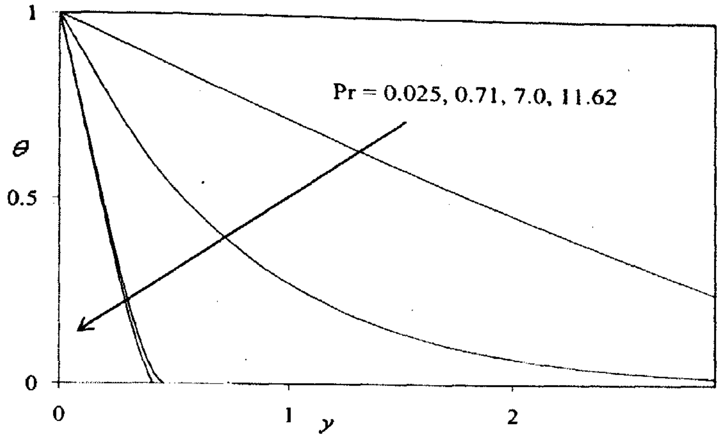

Figure 12. Temperature profiles for different values of Pr

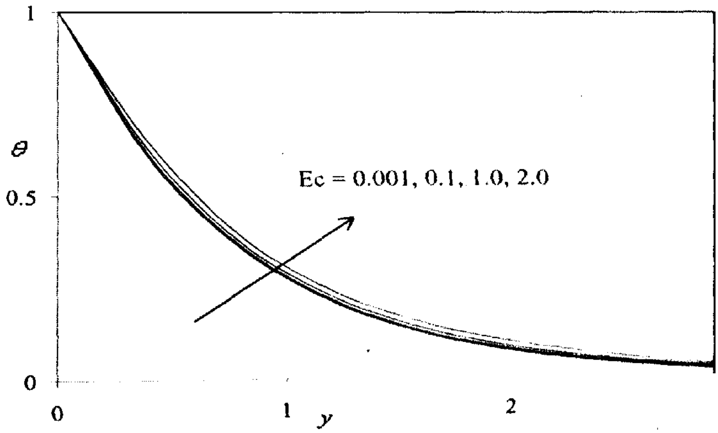

Figure 13. Temperature profiles for different values of Ec

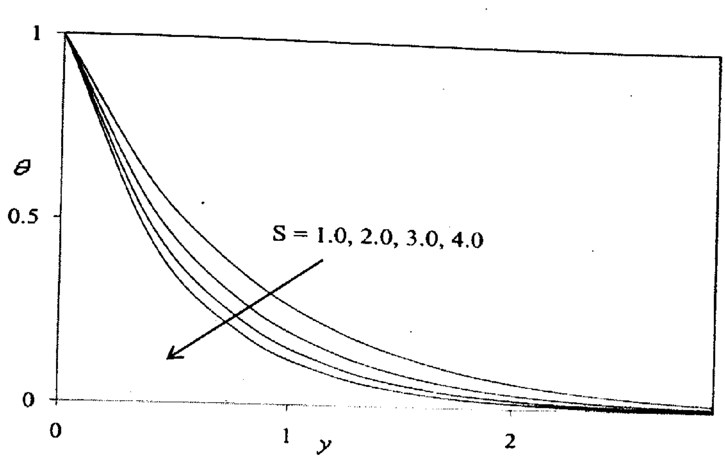

Figure 14. Temperature profiles for different values of S

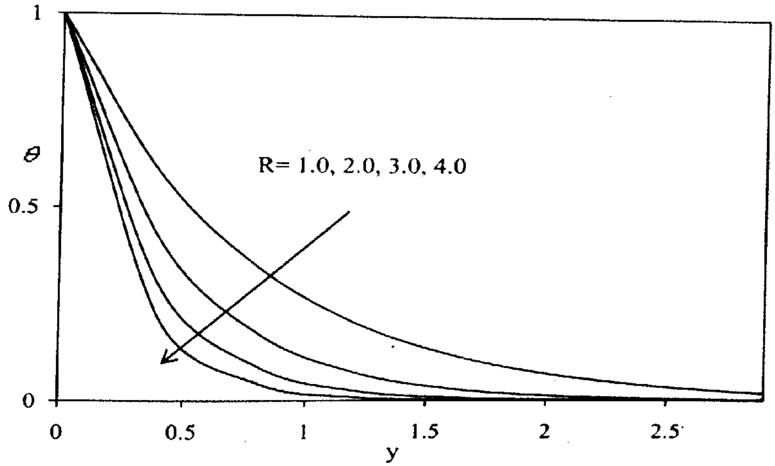

Figure 15. Temperature profiles for different values of R

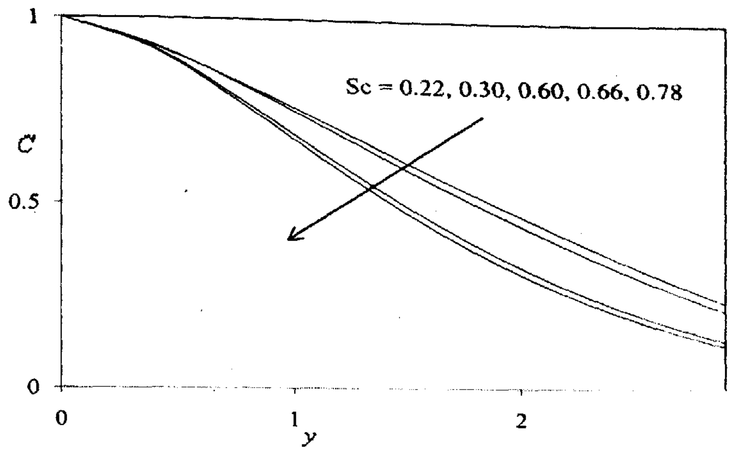

Figure 16. Temperature profiles for different values of *Sc*

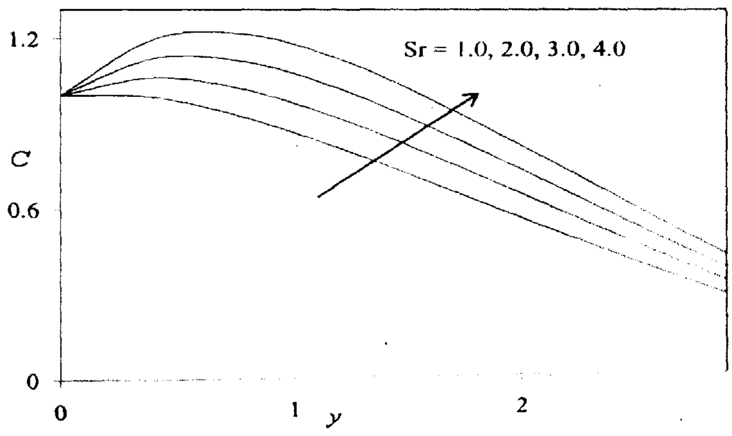

Figure 17. Temperature profiles for different values of *Sr*